

Journal Pre-proof

Performance improvement of EPDM and EPDM/Silicone rubber composites using modified fumed silica, titanium dioxide and graphene additives

Sohrab Azizi, Gelareh Momen, Claudiane Ouellet-Plamondon, Eric David



PII: S0142-9418(19)31449-7

DOI: <https://doi.org/10.1016/j.polymertesting.2019.106281>

Reference: POTE 106281

To appear in: *Polymer Testing*

Received Date: 19 August 2019

Revised Date: 19 November 2019

Accepted Date: 3 December 2019

Please cite this article as: S. Azizi, G. Momen, C. Ouellet-Plamondon, E. David, Performance improvement of EPDM and EPDM/Silicone rubber composites using modified fumed silica, titanium dioxide and graphene additives, *Polymer Testing* (2020), doi: <https://doi.org/10.1016/j.polymertesting.2019.106281>.

This is a PDF file of an article that has undergone enhancements after acceptance, such as the addition of a cover page and metadata, and formatting for readability, but it is not yet the definitive version of record. This version will undergo additional copyediting, typesetting and review before it is published in its final form, but we are providing this version to give early visibility of the article. Please note that, during the production process, errors may be discovered which could affect the content, and all legal disclaimers that apply to the journal pertain.

© 2019 Published by Elsevier Ltd.

Authors' accepted manuscript
Article published in *Polymer Testing*
<https://doi.org/10.1016/j.polymertesting.2019.106281>

© 2019. This manuscript version is made available under the CC-BY-NC-ND 4.0 license
<http://creativecommons.org/licenses/by-nc-nd/4.0/>

Performance Improvement of EPDM and EPDM/Silicone Rubber Composites Using Modified Fumed Silica, Titanium Dioxide and Graphene additives

Sohrab Azizi^{1*}, Gelareh Momen², Claudiane Ouellet-Plamondon¹, Eric David¹

¹ École de Technologie Supérieure (Université du Québec), 1100 Notre Dame St. W,
H3C 1K3, Montréal, QC, Canada

² Université du Québec à Chicoutimi (UQAC), 555 Boulevard de l'Université, Chicoutimi, QC G7H
2B1, Canada

Abstract

In this work, a polymeric composite was prepared from ethylene propylene diene monomer (EPDM) and silicone rubber (S) with additives of modified fumed silica (MFS), titanium dioxide (TiO₂) and graphene. The dielectric and thermal performances of the EPDM-based composites were studied. An increase in the dielectric constant and AC dielectric breakdown strength was observed for the EPDM rubber composites containing MFS, TiO₂, and graphene additives. In addition, the incorporation of the additives resulted in a significant increase in the thermal stability (~ 30–50 °C) and thermal conductivity (~ 7–35 %) of the composites. The combination of these various improvements gives suitable performance advantage to the polymeric composite for use in insulating applications.

Keywords: EPDM rubber; thermal stability; AC breakdown strength; insulating application.

1 Introduction

Many studies have been conducted in the development of high-voltage insulators possessing high electrical and thermal performances [1-5]. With the emergence of silicone rubber composites, the demand for conventional outdoor insulators, such as glass- or porcelain-based insulators has significantly reduced [6]. The incorporation of the inorganic-based additives, such as alumina trihydrate (ATH), TiO₂, and

* Correspondence to: Dr. Sohrab Azizi, E-mail: sohrab.azizi.1@ens.etsmtl.ca

Tel. +1 514 699 5484

Department of automation production engineering, École de technologie supérieure (ÉTS), Université du Québec, 1100 Notre-Dame St W, Montréal, QC H3C 1K3 Canada.

silica, in polymer compounds was found to be appropriate to design high voltage insulators with high thermal stability and electric breakdown strength [7]. However, the most common rubber compounds for high-voltage applications are common silicone rubber and ethylene propylene diene rubber (EPDM) [8]. In addition to possessing the appropriate electrical, thermal and mechanical properties, EPDM is a promising insulator due to its light weighting, ease-of-installation and handling properties [2, 9].

A better understanding of the initial properties of the rubber-based material is required in the development of the insulating materials. Outdoor insulating materials, such as silicon rubber-based composites, have received significant attention on the topics of resistance against ultra-violet (UV) oxidation, thermal aging, acid rain and dry band arcing, dielectric breakdown strength and mechanical cyclic loading [8]. In addition, it is known that a proper preparation technique is required for desirable insulating properties [10]. For this purpose, rubber compounds with low surface energy, such as silicone rubber or EPDM, with acceptable electrical, thermal and mechanical properties have been frequently investigated. For example, a blend of EPDM/polyimide rubber, compounded with nanosilica, exhibited a desirable improvement in thermal conductivity, as well as the thermal stability of the corresponding composites [11]. The blending of the micro- and nano-sized SiO_2 additives in EPDM and silicone rubber resulted in higher thermal stability and electrical performance [12]. Co-blending of micro- and nano-sized SiO_2 with EPDM rubber was also found to increase the resistance to corona discharge [13]. Significant improvement in the electrical and mechanical performance of EPDM rubber is reinforced by barium titanate where the treated barium titanate additives showed a better additives dispersion and compatibility than the non-treated one [14]. A remarkable increase in dielectric strength breakdown was reported for EPDM/silicone rubber with the addition of 1 wt% alumina trihydrate additive [15]. *In-situ* sol-gel processing of EPDM rubber and chemically treated silica with tetraethoxysilane with bis-[3-(triethoxysilyl)-propyl]-tetrasulfide as a coupling agent resulted in a strong interaction between the additive and rubber and a substantial increase in thermal stability of the composite [7]. Moreover, it has been shown that the incorporation of layered silica and organically modified montmorillonite featured better thermal stability and a slight increase of the dielectric constant in EPDM/silicone blend nanocomposites [16]. γ -Irradiation has been also claimed as an effective method to increase the thermal stability of the EPDM rubber composite compounded with micro- and nano-silica [3]. In addition, the dielectric constant of the irradiated EPDM composites was increased with the increase of the silica content [17]. The mechanism of UV accelerated surface degradation of the silicone rubber and EPDM loaded with alumina trihydrate has been studied which causes that EPDM is becoming less resistant to thermal degradation under UV weathering conditions than the silicone rubber composites in terms of hydrophobicity and surface resistivity [18].

As discussed, EPDM rubber is capable of withstanding bad weathering conditions at very low temperatures (~ -30 °C), with a significant elongation at break (~ 600 %) and good abrasion resistance [18, 19]. However, blending with silicone rubber can also improve UV resistance, aging resistance, resistance at high temperature and hydrophobicity [20-22]. Alumina trihydrate and silica reinforcement have frequently been studied in terms of electrical and thermal performances. Different techniques and strategies have been used to develop the properties of the EPDM rubber composites incorporating these inorganic additives. TiO_2 is an inorganic additive with a desirable self-cleaning property and suitable electrical and thermal properties was also studied with several silicone rubber composites [23-25]. The incorporation of graphene oxide in poly methyl methacrylate showed significant increase in thermal stability of PMMA composites [26]. The addition of reduced graphene oxide was found to enhance the thermal stability of the poly (n-butyl methacrylate) composite [27]. Graphene with exceptional electrical and thermal properties [28-30] featured noticeable improvement in electrical, thermal and mechanical properties of several rubber composites [31-33]. In some circumstances, rubber insulating materials such as silicone rubber compounded with a low quantity of conductive derivative graphite (~ 1 to 2 phr) demonstrated noticeable improvement in electrical performance and thermal stability [34, 35]. However, few studies have been carried out on EPDM rubber compounded with graphene.

In the present study, chemically modified fumed silica (MFS), TiO_2 and low contents of graphene were utilized to improve the electrical and thermal properties of EPDM and EPDM/S rubber composites. The morphology and homogeneity of the composites were observed. The chemical interactions of the inclusions with the rubber matrix were studied. The thermal stability and hydrophobicity of the composites were also investigated.

2 Materials, compounding, and characterization

2.1 Materials

Ethylene propylene diene monomer (VistalonTM 404) with mooney viscosity of 28 MU (based on ASTM D 1646) with an ethylene content of 45% and a density of 0.87 g.cm^{-3} at 25 °C was kindly provided by ExxonMobil. Polydimethylsiloxane diol (silicone rubber) (Elastosil@ R 401/60 S) with a density of $\sim 1.15 \text{ g cm}^{-3}$ at 20 °C and the mooney viscosity of 42 MU was provided by Wacker. Titanium (IV) dioxide (TiO_2), anatase grade with the specific surface area of 45-55 m^2/g and a density of 3.9 g cm^{-3} at 25 °C was purchased from Aldrich. Modified fumed silica (CAB-O-SIL TS-530) (Silanamine, 1,1,1-trimethyl-N-(trimethylsilyl)-, hydrolysis products with silica) with a density of $2.2\text{-}2.3 \text{ g cm}^{-3}$ was provided by Cabot. Graphene (GrapheneBlackTM 3X) with the primary particle size 1-2 μm and agglomerate moderate

particle size of D50= 38 μm and a bulk density of 0.18 g cm^{-3} was provided by NanoXplore. Dicumyl peroxide (DCP) was supplied by Aldrich. All materials were used as received.

2.2 Sample preparation

EPDM rubber gum, silicone rubber gum (S), TiO_2 , MFS, graphene (G), and DCP were intensively mixed in an internal mixer (Haake Rheomix OS) for 10 min with a screw speed of 100 rpm at 60 $^\circ\text{C}$. Several batches of composites (E/MFS-X, or E/ TiO_2 -X, X= part per hundred (phr)) were selected as shown in Table I. Then, all prepared composites were vulcanized using a hydraulic hot press (Accudyne Engineering & Equipment Company, Los Angeles, USA) at 165 $^\circ\text{C}$ mold temperature and 10 MPa load for 10 min. Subsequently, the cured composites were gradually cooled down to room temperature. It is worth mentioning that due to reaching a high viscosity during composite preparation, EPDM rubber was not possible to compound with 20 phr of the MFS additive.

Table I. The formula of the prepared composites.

Component	EPDM (phr)	S (phr)	MFS (phr)	TiO_2 (phr)	G (phr)	DCP (phr)
EPDM	100	-	-	-	-	0.7
S	-	100	-	-	-	0.7
EPDM/MFS_10	100	-	10	-	-	0.7
EPDM/MFS_10/G2	100	-	10	-	2	0.7
EPDM/ TiO_2 _20	100	-	-	20	-	0.7
EPDM/ TiO_2 _20/G2	100	-	-	20	2	0.7
EPDM/S/ TiO_2 _20	50	50	-	20	-	0.7
EPDM/S/ TiO_2 _20/G2	50	50	-	20	2	0.7

2.3 Characterization and measurements

The dielectric properties of the EPDM rubber composites were evaluated, from 10^{-1} to 10^5 Hz at room temperature. A disk-shaped sample with a thickness of ~ 2 mm and a diameter of 30 mm was sandwiched between the two electrodes and the formed capacitor was subjected to an AC applied voltage of 3 Vrms.

The electric breakdown strength of the EPDM rubber composite was evaluated using Baur electric breakdown tester. The experiment was conducted by the positioning of a flat disk of the sample with a thickness of ~ 2 -2.5 mm and a diameter of 10 mm in a mineral oil medium. According to ASTM D149-09(2013), 10 measurements with an increasing voltage of 0.5 kV s^{-1} were carried out.

The morphology of the EPDM rubber composites was imaged by a high-resolution electron microscope (Hitachi, SU-8230 FE-SEM, Japan). Each sample was immersed in liquid nitrogen and was cross-

sectionally cut by cryogenic microtoming. Then, the samples were coated by a 2 nm layer of platinum in a vacuumed chamber using a turbo-pumped sputter coater/carbon coater (Q150T, Guelph, Canada).

Any chemical interaction between the inclusion and the medium rubber was evaluated by FT-IR experiment over the wavenumbers from 400 to 4000 cm^{-1} . Characterization was carried out in absorbance mode with a PerkinElmer FT-IR Spectrometer.

Thermogravimetric analysis (TGA) was conducted using coupled TGA-FTIR (STA 8000 instrument (PerkinElmer)) tester by a ~ 10 to 15 mg test specimen under a constant flow rate of 70 ml of nitrogen gas. Heating was carried out from 50 to 800 $^{\circ}\text{C}$ with a rising rate of 30 $^{\circ}\text{C min}^{-1}$. The released elements from the TGA instrument were passed through a tube to the FT-IR analyzer. FT-IR spectra were recorded over the wavenumbers of 400-4000 cm^{-1} . Thermogravimetric analysis (TGA) under air atmosphere was also conducted with a heating ramp of 30 $^{\circ}\text{C min}^{-1}$ and 50 cc/min air flow over the temperature range of 50-650 $^{\circ}\text{C}$.

The thermal conductivity of the composites was evaluated using a guarded heat flux meter (C-Therm Technologies) with a disk-shaped sample with a thickness of ~ 2 mm and a diameter of 20 mm.

The hydrophobicity of the EPDM rubber composites was evaluated by water-contact-angle measurement using VCA optima (Ast Products Inc.). To measure the contact angle, firstly, the surface of the test specimens was carefully washed with isopropanol and dried with instrument air. The measurement was carried out at room temperature, capturing 5 photos of the 5 μl dripped ultrapure deionized water droplets on the surface of the test specimens at different locations.

3 Results and discussion

3.1 Dielectric properties

The dielectric responses of EPDM rubber composites, dielectric constant and dissipation factor are shown in Figure. 1a and Figure. 1b, respectively. Both EPDM and silicone rubber showed low dielectric losses and a frequency-independent low dielectric constant due to their non-polar polymer backbone. The dielectric properties of the composites depend on the intrinsic properties of the materials such as the permittivity and the electrical conductivity [15, 36]. In heterogeneous materials such as composites containing additives, the interfacial polarization or Maxwell–Wagner–Sillars effect [30, 37-41] is commonly observed in the intermediate frequency range, given the rise of a broad relaxation peak. The addition of TiO_2 was found to significantly increase the dielectric constant of the EPDM rubber, as well as the dissipation factor in the frequency ranges of 10^1 – 10^4 Hz, due to the interfacial polarization at the surface of the inclusions. This effect was found to be improved when the polymeric matrix is an EPDM/S

blend, possibly due to the selective location of the inorganic additives [14, 17, 38, 42]. On the other hand, the dielectric loss of the EPDM rubber composites with either MFS or MFS/G additives showed no significant changes.

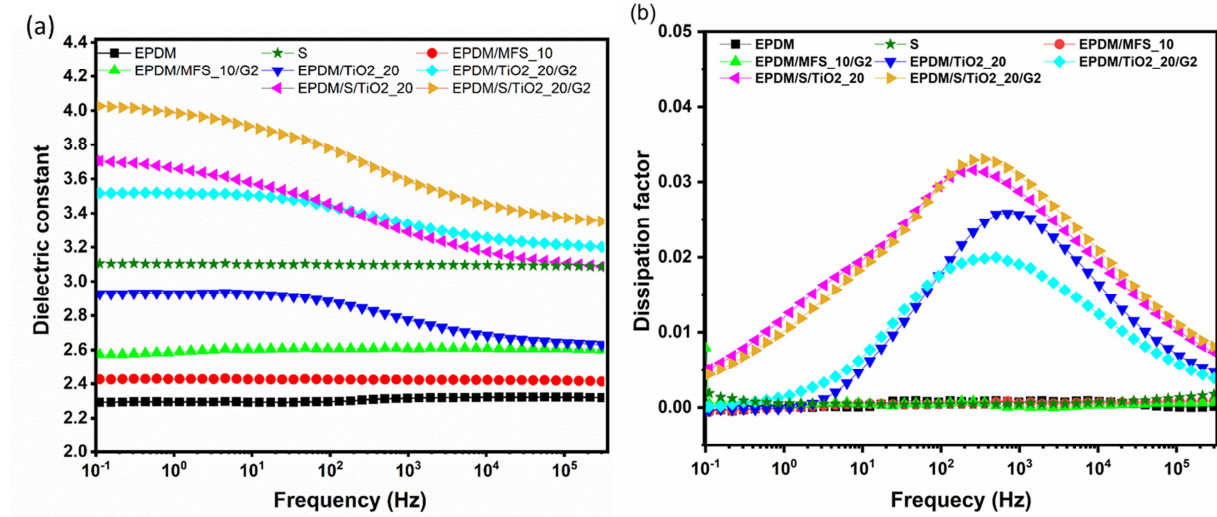


Figure. 1. Dielectric properties, (a) dielectric constant and (b) dissipation factor, of the EPDM rubber and its corresponding composites blended with silicone rubber at room temperature.

3.2 AC dielectric breakdown strength

The AC dielectric breakdown strength of the EPDM rubber composites is shown in Figure 2 and the Weibull parameters are listed in Table II, which were calculated according to the Eq. 1:

$$P(E) = 1 - \exp\left[-\left(\frac{E}{\alpha}\right)^\beta\right] \quad \text{Eq. 1}$$

where $P(E)$ is the cumulative failure probability at an electric field, α is the characteristic breakdown strength, for which 63.2 % of the test specimens have failed at that certain electric field, and β is related to the width of the distribution of the data [43]. As can be seen from the Weibull distribution plots, loading of 10 phr of the MFS additive slightly increased the characteristic breakdown strength by 16%, while 2 phr of graphene additive was further loaded to EPDM/MFS_10, the dielectric breakdown strength of the composite increased by 23 % than the virgin EPDM rubber. The addition of 20 phr of TiO₂ additive was led to relatively close values of the dielectric breakdown strength of the EPDM rubber. However, as 2 phr of graphene was added to EPDM/TiO₂_20 composite, the breakdown strength improved by 23% over the vulcanized EPDM rubber, potentially due to the trapping of the charge carriers at the graphene/polymer boundaries [37]. In comparison, TiO₂ showed less efficiency in improving the dielectric breakdown strength compared to the MFS additive, likely because of the absorbed moisture by

the TiO₂ particles which acted as a defect in the composite structure [44]. The EPDM/S/ TiO₂_20 and EPDM/S/ TiO₂_20/G2 rubber composites showed an increase in the dielectric breakdown strengths of 30 and 34%, respectively, over the EPDM vulcanized rubber. A summary of the dielectric breakdown strength of several EPDM and silicone rubber composites that have been investigated is shown in Table II. A dielectric breakdown of 21.1 to 22.2 kV/mm was obtained for the EPDM rubber composites containing various forms of SiO₂. It is worth mentioning that fabrication method had significant impact on the dielectric breakdown strength of the composites. Moreover, our findings revealed that a combination of EPDM/silicone rubber composite with 20 phr of TiO₂ and 2 phr of graphene resulted in a relatively high dielectric breakdown strength compared to its counterparts.

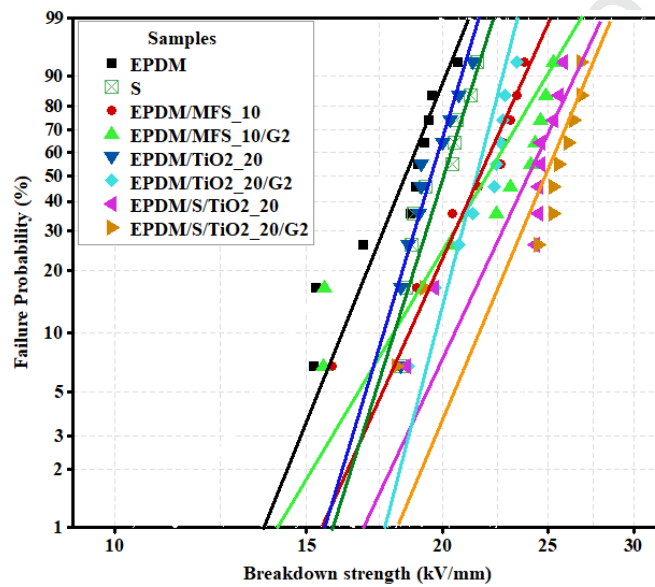


Figure 2. Weibull distribution plot of the electric breakdown of EPDM rubber and its composites.

Table II. Summary of Weibull parameters of current composites containing MFS, TiO₂, graphene and several former studies.

Sample	Shape (β)	E_{BD} (kV/mm)	Reference
EPDM	13.95	19.02	Our work
S	19.68	20.32	Our work
EPDM/MFS_10	12.75	22.22	Our work
EPDM/MFS_10/G2	9.10	23.39	Our work
EPDM/TiO ₂ _20	20.03	19.96	Our work
EPDM/TiO ₂ _20/G2	20.53	22.28	Our work
EPDM/S/TiO ₂ _20	16.48	24.66	Our work
EPDM/S/TiO ₂ _20/G2	13.38	25.56	Our work
Silicone rubber/ ATH_15 wt%	-	22.5	[45]
Silicone rubber/15 wt% of modified alumina with vinyl trimethoxysilane	-	24.1	[45]
EPDM/micro SiO ₂ _20 wt%	-	21.1	[12]

EPDM/nano SiO ₂ _5 wt%	-	22.2	[12]
EPDM/ micro SiO ₂ _15 wt%/ nano SiO ₂ _5 wt%	-	24.5	[12]
Silicone rubber/ ATH	--	18.9	[46]
Silicone rubber/ irregular SiO ₂	-	24.9	[46]
Silicone rubber/ sphere SiO ₂	-	24.8	[46]
EPDM_50 vol %/ Silicone_ 50 vol %/ ATH_5vol %	-	25.6	[15]

3.3 SEM imaging

Figure 3 shows the SEM images of the EPDM, silicone rubber and their corresponding composites with additives of MFS, TiO₂ and graphene. The SEM micrograph of EPDM/MFS_10 showed some aggregates of ~ 10–15 μm, indicating inadequate additive dispersion within the rubber composite, whereas, adding 2 phr of graphene into EPDM/MFS_10 was led to a better homogenous morphology with well-dispersed and distributed inclusions (Figure 3c and Figure 3d). EPDM rubber composite with 20 phr TiO₂ was found to show a uniform morphology (Figure 3e), and adding 2 phr of graphene to EPDM/TiO₂-20 led to further additive density in the morphology as it can be seen in Figure 3f. The blending of EPDM with silicone rubber followed by the inclusion of 20 phr of TiO₂ and 2 phr of graphene resulted in a different morphology, featuring the phase separation between two immiscible polymers (Figure 3g and Figure 3h). Some agglomerates of the graphene particles were also observed in Figure 3h.

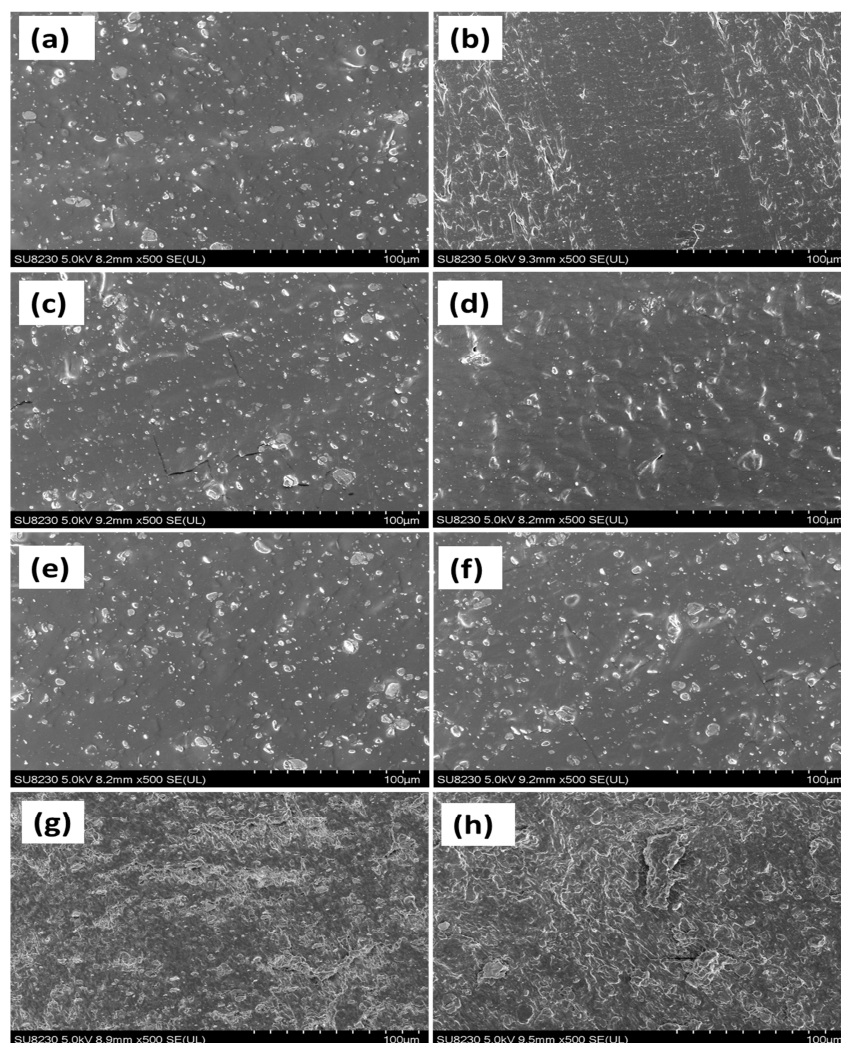


Figure 3. SEM images of (a) EPDM rubber, (b) silicone rubber, (c) EPDM/MFS_10 (d) EPDM/MFS_10/G2, (e) EPDM/TiO₂_20, (f) EPDM/TiO₂_20/G2, (g) EPDM/S/TiO₂_20 and (h) EPDM/S/TiO₂_20/G2.

3.4 FT-IR spectroscopy

The FT-IR spectra of the EPDM rubber composites are shown in Figure 4. As can be seen, two strong absorption peaks are identified at 2923 and 2850 cm^{-1} wavelength, which are designated as the C–H stretching vibration [47]. At wavenumbers of 720, 1376 and 1460 cm^{-1} , three adsorption peaks were detected, which are assigned to the $-\text{CH}_2$ stretching, and $-\text{CH}_3$ and $-\text{CH}_2$ bending, respectively [7]. The absorption peaks at 2968 cm^{-1} , 1265 cm^{-1} and 1000-1125 cm^{-1} were also observed in silicone rubber spectra, which were attributed to the characteristic stretching vibration of C–H, Si–C and Si–O–Si, respectively [48]. A wide absorption peak between a range of 3500-3750 cm^{-1} was appeared for the

spectra of the EPDM rubber composites, shown the $-OH$ groups [49]. The absorbance peak of the EPDM rubber was used as the reference in order to compare the intensity of the absorption peak of the other counterparts and the results are listed in Table III. In principle, the spectral demonstration of the EPDM and silicone rubber composites were observed to be similar to those of the vulcanized EPDM and silicone rubber matrix with lower intensity in the absorbance peaks. This indicates that the curing process was comparable between the different EPDM and silicone rubber composites.

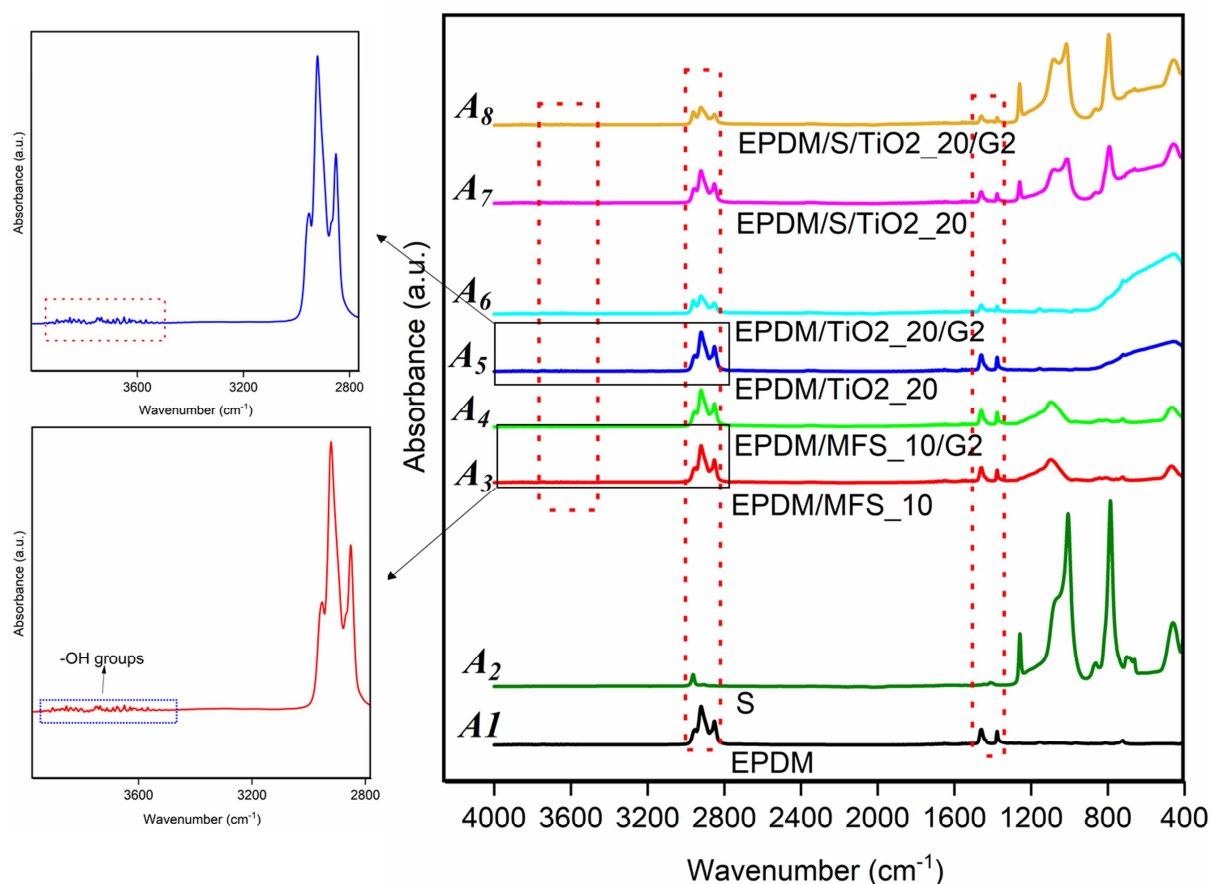


Figure 4. FT-IR spectra of EPDM, silicone rubber and its corresponding rubber composites.

Table III. The relative intensity of the absorbance peaks of EPDM rubber composites with respect to the EPDM rubber at several wavenumbers.

Relative intensity	Wavenumber (cm^{-1})			
	2953	2921	1460	1377
$\frac{A_3}{A_1}$	0.95	0.96	0.96	0.92
$\frac{A_4}{A_1}$	0.99	1.01	0.98	0.99
$\frac{A_5}{A_1}$	0.98	1.01	0.99	0.99
$\frac{A_6}{A_1}$	0.79	1.02	0.67	0.69
$\frac{A_7}{A_1}$	0.98	0.86	0.78	0.76
$\frac{A_8}{A_1}$	0.99	0.51	0.67	0.69

3.5 Thermal stability and TGA-FTIR analysis

To investigate the thermal stability and the mechanism of degradation in the EPDM and silicone rubber and their corresponding composites, TGA-FTIR analysis was conducted. The thermal stability of the EPDM rubber composites is shown in Figure 5. For a further understanding of the mechanism of the degradation and decomposition of the EPDM rubber-based composites, the 3D histogram of TGA-FTIR analysis is shown in Figure 6. Thermal stability in outdoor insulating materials is a vital parameter, which can hinder or suppress several destructive phenomena, such as dry band arcing or surface erosion. Thermal aging as the result of dry band arcing may change the inherent hydrophobicity of the insulator and consequently render the material hydrophilic, which significantly decreases the insulator performance. Thus, the addition of inorganic additives with excellent thermal stability to rubbers is expected to improve the materials' thermal performance [50, 51]. Moreover, inorganic additives in rubber insulating composites can mitigate the leakage current and corona exposure surface erosion which ultimately leads to a higher performance [37]. According to the TGA plots under air atmosphere (Figure 5a), EPDM rubber composites have gained slightly weight due to oxidation reaction at temperature range of 120 to 300 °C. EPDM rubber composites featured decomposition commencing ~ 350 °C under air atmosphere while under nitrogen atmosphere were stable up to ~ 400 °C, since no significant weight loss was observed below that temperature (observed in TGA plot under nitrogen atmosphere, Figure 5b). This can be attributed to the physical interactions at the interface layer of the polymer-additives [52, 53]. This was in good agreement with the TGA-FTIR histograms, for which no detectable FT-IR peak was observed below ~ 400 °C (Figure 6). The degradation of the EPDM rubber and its corresponding composites were observed to start around 350 and 400 °C (for air and nitrogen atmosphere, respectively),

and all samples without silicone rubber experienced a one-step weight loss. The blending of EPDM rubber with silicone rubber and the addition of MFS, TiO₂, and graphene led to an increase in thermal stability, where a maximum value of 448 °C (at 5 % wt. loss) was observed for the EPDM/S/TiO₂_20/G2 (Table IV). Most likely, the increase in thermal stability of the EPDM/S/TiO₂_20/G2 rubber composites is due to the formation of a TiO₂ network, followed by the integration of graphene particles which resulted in a strong physical interaction between polymer and additives [52, 54-58]. Both rubber composites, the EPDM/S/TiO₂_20 and EPDM/S/TiO₂_20/G2, experienced a second weight loss between ~ 480-580 and 500-750 °C (for air and nitrogen atmosphere, respectively) which is related to the degradation of the silicone rubber chains. This second weight loss (observed in TGA plot under nitrogen atmosphere, Figure 5b) results in the detection of an absorption peak at 3013 cm⁻¹, related to the methane generated during the decomposition process of silicone rubber (Figure 6g and Figure 6h) [59, 60]. In order to compare the thermal stability of the EPDM and silicone rubber composites, a summary of thermal properties of several composites that have been formerly studied is shown in Table IV. Overall, the combination of a low quantity of graphene additive was found to increase the thermal degradation of the rubber insulating composite.

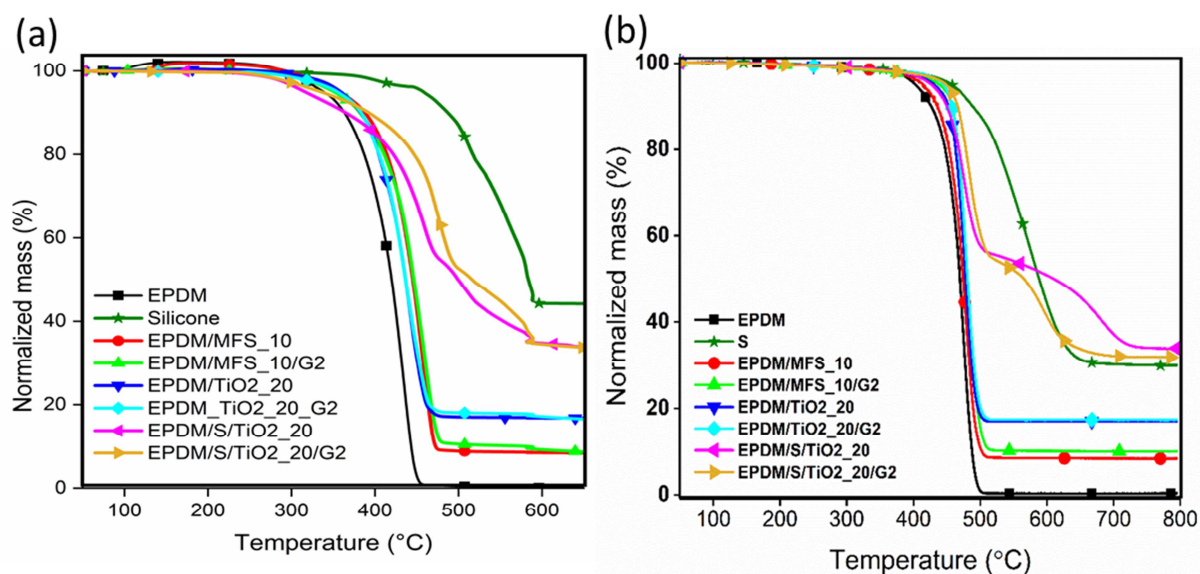


Figure 5. TGA plot of EPDM and silicone rubber composite under (s) air atmosphere, (b) nitrogen atmosphere.

Table IV. Summary of TGA results of current research and several studies of EPDM and silicone rubber composites.

Sample	Atmosphere condition		T _{5%} (°C)		T _{50%} (°C)		Ash (wt%)	Reference
			air	N2	air	N2		
EPDM	air	N2	343	403	420	470	0.3	Our work
S	air	N2	338	457	581	588	30	Our work
EPDM/MFS_10	air	N2	346	414	451	474	8.3	Our work
EPDM/MFS_10/G2	air	N2	351	438	453	481	9.9	Our work
EPDM/TiO ₂ _20	air	N2	350	431	448	478	17	Our work
EPDM/TiO ₂ _20/G2	air	N2	353	444	451	481	18.1	Our work
EPDM/S/ TiO ₂ _20	air	N2	303	426	503	610	34	Our work
EPDM/S/ TiO ₂ _20/G2	air	N2	331	448	512	570	32.3	Our work
Micro- aluminum nitride _40 wt%/ silicone rubber	Not available		392		Not achieved		-	[61]
Nano-SiO ₂ -7 wt%/Silicone rubber	Not available		483		Not achieved		-	[61]
Micro- aluminum nitride -25 wt%/nano-SiO ₂ -5 wt% / silicone rubber	Not available		514		Not achieved		-	[61]
Acrylonitrile butadiene styrene /EPDM	N2		390.7		442		-	[32]
Acrylonitrile butadiene styrene /EPDM/graphene- 8 wt% (melt mixing)	N2		389		440		-	[32]
Acrylonitrile butadiene styrene /EPDM/graphene- 8 wt% (wet premixing)	N2		375.7		440		-	[32]
Acrylonitrile butadiene styrene /EPDM/graphene- 8 wt% (dried premixing)	N2		382.1		442		-	[32]
High temperature vulcanized silicone rubber	N2		465		578		-	[62]
High temperature vulcanized silicone rubber/ Sodium montmorillonite_5 wt%	N2		472		585		-	[62]
High temperature vulcanized silicone rubber/ Sodium montmorillonite_5 wt%/carbon fiber _1 wt%	N2		477		589		-	[62]
High temperature vulcanized silicone rubber/ Modified sodium montmorillonite_5 wt%	N2		485		602		--	[62]
High temperature vulcanized silicone rubber/ Modified sodium montmorillonite_5 wt%/carbon fiber_1 wt%	N2		490		613		-	[62]
EPDM	N2		426		454		-	[7]
EPDM/SiO ₂ -10 wt%	N2		420		452		-	[7]
EPDM/SiO ₂ -20 wt%	N2		435		463		-	[7]
EPDM/SiO ₂ -30 wt%	N2		436		469		-	[7]

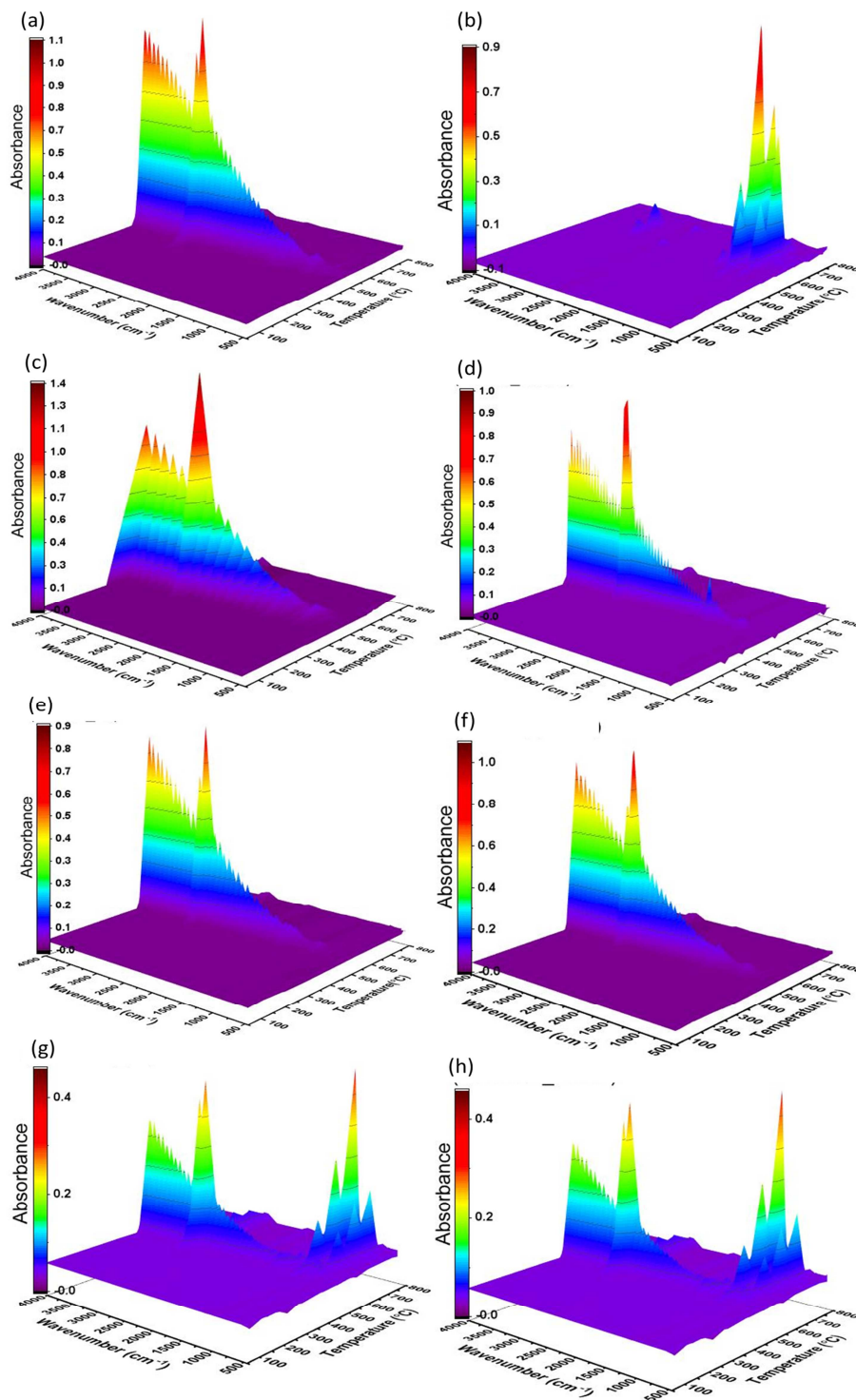


Figure 6. 3D histograms of TGA-FTIR analysis of (a) EPDM, (b) silicone rubber, (c) EPDM/MFS_10, (d) EPDM/MFS_10/G2, (e) EPDM/TiO₂_20 (f) EPDM/TiO₂_20/G2, (g) EPDM/S/ TiO₂_20 and (h) EPDM/S/ TiO₂_20/G2 during the degradation at high temperature.

3.6 Thermal conductivity

The variation of the thermal conductivity for the various samples is shown in Figure 7. Loading of MFS, TiO_2 and graphene additives in EPDM and EPDM/S rubbers resulted in a higher thermal conductivity for all of the composites. The highest values of thermal conductivity were achieved for the EPDM composites containing TiO_2 . The further addition of graphene did not appear to affect the composites' thermal conductivity. Multiple parameters can influence directly or indirectly the thermal conductivity of the composites. For example, particle size and the intrinsic thermal conductivity of the inclusions play a significant role in the conductivity of the composites [63-65]. Crosslinking has a considerable impact on the conductivity of rubber composites by bridging polymer chains and providing a higher intra-atomic connection. The higher the crosslinking, the greater thermal conductivity in the composites. In addition, the polymer morphology, such as chain alignment that can occur during processing, can significantly increase the thermal conductivity [66]. Similarly, additive orientation and the formation of pathways or connected network can also increase the thermal conductivity. The combination of the 3D additives (MFS or TiO_2) with 2D graphene layers can be an effective strategy to increase the thermal conductivity [67-69]. Therefore, the incorporation of high thermal conductivity additives and the formation of conductive pathways in the composite structure, as well as the vulcanization of rubber chains caused increases in the thermal conductivity of the rubber composites simultaneously.

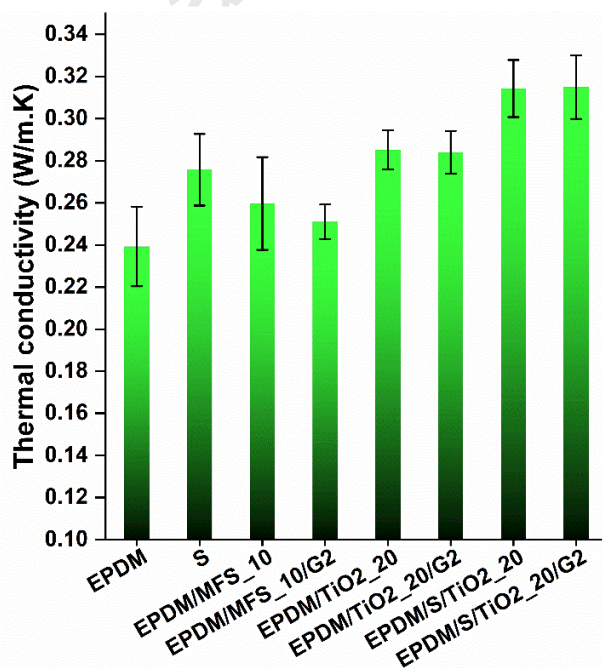


Figure 7. Thermal conductivity of EPDM rubber composites including MFS, TiO_2 , and graphene additives.

3.7 Static water contact angle measurement

The static water contact angle (CA) of the EPDM rubber composites with the standard deviation (SD) are shown in Figure 8. As illustrated, the EPDM rubber showed a contact angle of 91° , which is lower than the water contact angle of silicone rubber (108°). Adding 10 phr of MFS to EPDM rubber was found to slightly increase (5°) the water contact angle. The addition of 2 phr of graphene to EPDM/MFS_10 was led to a small increase (8.8°) in hydrophobicity (with respect to vulcanized EPDM rubber) potentially due to a greater surface roughness of the composite [70, 71]. The addition of 20 phr of TiO_2 is led to a significant decrease in hydrophobicity, which can be interpreted by the hydrophilic nature of the TiO_2 additive [71]. However, the blending of the EPDM/ TiO_2 _20 rubber composite with the hydrophobic silicone rubber improved the contact angle, for which an average contact angle of 104.4° was obtained. In the case of the MFS composite, the addition of 2 phr of graphene additive to EPDM/S/ TiO_2 _20 did not significantly change the static water contact angle.

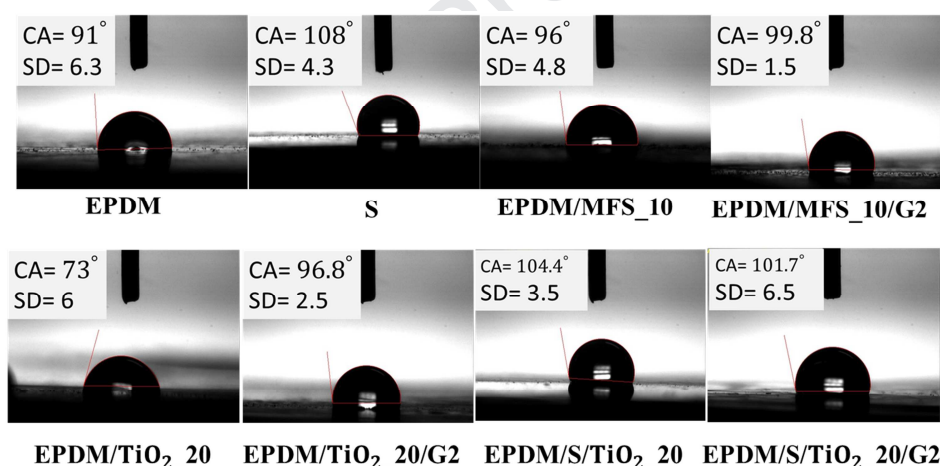


Figure 8. The average static water contact angle of EPDM, silicone rubber and their corresponding rubber composites.

4 Conclusions

The compounding of EPDM rubber with MFS, TiO_2 and graphene additives *via* mechanical mixing resulted in the improvement of the electrical properties, such as the AC dielectric breakdown strength. In addition, loading of inorganic fillers of MFS, TiO_2 as well as graphene led to an increase ($\sim 30\text{--}50^\circ\text{C}$) in the thermal stability of the engineered EPDM-based composites. The simultaneous analysis of thermal degradation of the composites by TGA-FTIR technique revealed details of the rubber decomposition

process. The inclusion of thermally conductive graphene, as well as inorganic additives such as MFS and TiO₂, was found to raise the thermal conductivity of the composites. EPDM rubber composites with MFS, TiO₂ additives and low-content of graphene yields an appropriate thermal and electrical performance to the compounded composites for use in outdoor insulating applications.

Acknowledgment

The authors would like to thank Dr. Nima Moghimian and Dr. Seyed Milad Madinehei for their kind collaboration, as well as financial support by Natural Sciences and Engineering Research Council of Canada. The authors also acknowledge Mr. Michael Di Mare for his worthwhile collaboration.

Conflict of interest

There are no conflicts of interest among the manuscript's authors.

References

- [1] A.M. Pourrahimi, T.A. Hoang, D. Liu, L.K. Pallon, S. Gubanski, R.T. Olsson, U.W. Gedde, M.S. Hedenqvist, Highly efficient interfaces in nanocomposites based on polyethylene and ZnO nano/hierarchical particles: A novel approach toward ultralow electrical conductivity insulations, *Adv. Mater. Processes*, 28 (2016) 8651-8657.
- [2] P. Pourmand, L. Hedenqvist, A.M. Pourrahimi, I. Furó, T. Reitberger, U.W. Gedde, M. Hedenqvist, Effect of gamma radiation on carbon-black-filled EPDM seals in water and air, *Polym. Degrad. Stab.*, 146 (2017) 184-191.
- [3] D. Liu, A. Hoang, A.M. Pourrahimi, L.H. Pallon, F. Nilsson, S. Gubanski, R.T. Olsson, M.S. Hedenqvist, U.W. Gedde, E. Insulation, Influence of nanoparticle surface coating on electrical conductivity of LDPE/Al₂O₃ nanocomposites for HVDC cable insulations, *IEEE Transactions on Dielectrics*, 24 (2017) 1396-1404.
- [4] L. Pallon, A. Hoang, A. Pourrahimi, M.S. Hedenqvist, F. Nilsson, S. Gubanski, U. Gedde, R.T. Olsson, The impact of MgO nanoparticle interface in ultra-insulating polyethylene nanocomposites for high voltage DC cables, *Journal of Materials Chemistry A*, 4 (2016) 8590-8601.
- [5] F. Nilsson, M. Karlsson, L. Pallon, M. Giacinti, R.T. Olsson, D. Venturi, U.W. Gedde, M.S. Hedenqvist, Influence of water uptake on the electrical DC-conductivity of insulating LDPE/MgO nanocomposites, *Compos. Sci. Technol.*, 152 (2017) 11-19.
- [6] C. Zhou, L. Yu, W. Luo, Y. Chen, H. Zou, M. Liang, Ablation properties of aluminum silicate ceramic fibers and calcium carbonate filled silicone rubber composites, *J. Appl. Polym. Sci.*, 132 (2015).
- [7] T. Mokhothu, A. Luyt, M. Messori, Reinforcement of EPDM rubber with in situ generated silica particles in the presence of a coupling agent via a sol-gel route, *Polym. Test.*, 33 (2014) 97-106.

- [8] B.H. Youn, C.S. Huh, Surface degradation of HTV silicone rubber and EPDM used for outdoor insulators under accelerated ultraviolet weathering condition, *Ieee Transactions on Dielectrics and Electrical Insulation*, 12 (2005) 1015-1024.
- [9] H. Khan, M. Amin, M. Ali, M. Iqbal, M. Yasin, C. Sciences, Effect of micro/nano-SiO₂ on mechanical, thermal, and electrical properties of silicone rubber, epoxy, and EPDM composites for outdoor electrical insulations, *Turkish Journal of Electrical Engineering & Computer Sciences*, 25 (2017) 1426-1435.
- [10] H. Xu, L.X. Gong, X. Wang, L. Zhao, Y.B. Pei, G. Wang, Y.J. Liu, L.B. Wu, J.X. Jiang, L.C. Tang, Influence of processing conditions on dispersion, electrical and mechanical properties of graphene-filled-silicone rubber composites, *Composites Part a-Applied Science and Manufacturing*, 91 (2016) 53-64.
- [11] S. Singh, P. Guchhait, G. Bandyopadhyay, T. Chaki, Manufacturing, Development of polyimide–nanosilica filled EPDM based light rocket motor insulator compound: influence of polyimide–nanosilica loading on thermal, ablation, and mechanical properties, *Composites Part A: Applied Science*, 44 (2013) 8-15.
- [12] H. Khan, M. Amin, M. Yasin, M. Ali, A. Ahmad, Effect of hybrid-SiO₂ particles on characterization of EPDM and silicone rubber composites for outdoor high-voltage insulations, *J. Polym. Eng.*, 37 (2017) 671-680.
- [13] M.T. Nazir, B. Phung, M. Hoffman, E. Insulation, Performance of silicone rubber composites with SiO₂ micro/nano-filler under AC corona discharge, *IEEE Transactions on Dielectrics*, 23 (2016) 2804-2815.
- [14] J. Su, J. Zhang, Remarkable enhancement of mechanical and dielectric properties of flexible ethylene propylene diene monomer (EPDM)/barium titanate (BaTiO₃) dielectric elastomer by chemical modification of particles, *RSC Advances*, 5 (2015) 78448-78456.
- [15] M. Fairus, N.S. Mansor, M. Hafiz, M. Kamarol, M. Mariatti, Investigation on dielectric strength of alumina nanofiller with SiR/EPDM composites for HV insulator, 2015 IEEE 11th International Conference on the Properties and Applications of Dielectric Materials (ICPADM), IEEE, 2015, pp. 923-926.
- [16] H. Acharya, S.K. Srivastava, EPDM/Silicone Blend Layered Silicate Nanocomposite by Solution Intercalation Method: Morphology and Properties, *Polym. Compos.*, 35 (2014) 1834-1841.
- [17] M. Madani, Effect of silica type and concentrations on the physical properties of EPDM cured by γ -irradiation, *Mol. Phys.*, 106 (2008) 849-857.
- [18] M. Rallini, I. Puri, L. Torre, M. Natali, Thermal and ablation properties of EPDM based heat shielding materials modified with density reducer fillers, *Composites Part a-Applied Science and Manufacturing*, 112 (2018) 71-80.
- [19] A. De Almeida, L. Chazeau, G. Vigier, G. Marque, Y. Goutille, Ultimate and toughness properties of γ -irradiated EPDM, *Eur. Polym. J.*, 97 (2017) 178-187.
- [20] B. Sun, Z. Du, H. Cao, L. Du, W. Yu, Oxidation□grafting surface modification of waste silicone rubber composite insulator powder: Characterizations and properties of EPDM/modified waste powder composites, *J. Appl. Polym. Sci.*, 134 (2017) 45438.

- [21] R. Deepalaxmi, V. Rajini, Performance evaluation of gamma irradiated SiR-EPDM blends, *Nucl. Eng. Des.*, 273 (2014) 602-614.
- [22] S. Kole, S. Roy, A.K. Bhowmick, Interaction between Silicone and Epdm Rubbers through Functionalization and Its Effect on Properties of the Blend, *Polymer*, 35 (1994) 3423-3426.
- [23] M. Bleszynski, M. Kumosa, Aging resistant TiO₂/silicone rubber composites, *Compos. Sci. Technol.*, 164 (2018) 74-81.
- [24] Z.-M. Dang, Y.-J. Xia, J.-W. Zha, J.-K. Yuan, J. Bai, Preparation and dielectric properties of surface modified TiO₂/silicone rubber nanocomposites, *Mater. Lett.*, 65 (2011) 3430-3432.
- [25] M. Di, S. He, R. Li, D. Yang, Resistance to proton radiation of nano-TiO₂ modified silicone rubber, *Nuclear Instruments Methods in Physics Research Section B: Beam Interactions with Materials*, 252 (2006) 212-218.
- [26] M. Wåhlander, F. Nilsson, A. Carlmark, U.W. Gedde, S. Edmondson, E. Malmström, Hydrophobic matrix-free graphene-oxide composites with isotropic and nematic states, *Nanoscale*, 8 (2016) 14730-14745.
- [27] C. Cobo Sánchez, M. Wåhlander, M. Karlsson, D.C. Marin Quintero, H. Hillborg, E. Malmström, F. Nilsson, Characterization of Reduced and Surface-Modified Graphene Oxide in Poly (Ethylene-co-Butyl Acrylate) Composites for Electrical Applications, *Polymers*, 11 (2019) 740.
- [28] A. Akbari, P. Sheath, S.T. Martin, D.B. Shinde, M. Shaibani, P.C. Banerjee, R. Tkacz, D. Bhattacharyya, M. Majumder, Large-area graphene-based nanofiltration membranes by shear alignment of discotic nematic liquid crystals of graphene oxide, *Nature communications*, 7 (2016) 10891.
- [29] F. Razmjooei, K.P. Singh, D.S. Yang, W. Cui, Y.H. Jang, J.S. Yu, Fe-Treated Heteroatom (S/N/B/P)-Doped Graphene Electrocatalysts for Water Oxidation, *Acs Catalysis*, 7 (2017) 2381-2391.
- [30] S. Azizi, C. Ouellet-Plamondon, P.N. Tri, M. Fréchette, E. David, Electrical, thermal and rheological properties of low-density polyethylene/ethylene vinyl acetate/graphene-like composite, *Composites Part B: Engineering*, (2019) 107288.
- [31] L. Valentini, S.B. Bon, M.A. Lopez-Manchado, R. Verdejo, L. Pappalardo, A. Bolognini, A. Alvino, S. Borsini, A. Berardo, N.M. Pugno, Synergistic effect of graphene nanoplatelets and carbon black in multifunctional EPDM nanocomposites, *Compos. Sci. Technol.*, 128 (2016) 123-130.
- [32] F. Wang, Y. Zhang, B.B. Zhang, R.Y. Hong, M.R. Kumar, C.R. Xie, Enhanced electrical conductivity and mechanical properties of ABS/EPDM composites filled with graphene, *Composites Part B-Engineering*, 83 (2015) 66-74.
- [33] E. Shamsaei, F.B. de Souza, X.P. Yao, E. Benhelal, A. Akbari, W.H. Duan, Graphene-based nanosheets for stronger and more durable concrete: A review, *Construction and Building Materials*, 183 (2018) 642-660.
- [34] Z. Wang, J. Nelson, H. Hillborg, S. Zhao, L. Schadler, Nonlinear conductivity and dielectric response of graphene oxide filled silicone rubber nanocomposites, 2012 Annual Report Conference on Electrical Insulation and Dielectric Phenomena, IEEE, 2012, pp. 40-43.

- [35] Y. Song, J. Yu, L. Yu, F.E. Alam, W. Dai, C. Li, N. Jiang, Enhancing the thermal, electrical, and mechanical properties of silicone rubber by addition of graphene nanoplatelets, *Materials & Design*, 88 (2015) 950-957.
- [36] S. Azizi, M. Azizi, M. Sabetzadeh, The Role of Multiwalled Carbon Nanotubes in the Mechanical, Thermal, Rheological, and Electrical Properties of PP/PLA/MWCNTs Nanocomposites, *Journal of Composites Science*, 3 (2019) 64.
- [37] T. Tanaka, A.S. Vaughan, Tailoring of nanocomposite dielectrics: from fundamentals to devices and applications, Pan Stanford 2016.
- [38] S. Azizi, C. Ouellet-Plamondon, E. David, M. Fréchet, Electrical and thermal properties of low-density polyethylene/graphene-like composite, *Electrical Insulation and Dielectric Phenomenon (CEIDP), 2017 IEEE Conference on, IEEE, 2017*, pp. 517-520.
- [39] S. Kashi, R.K. Gupta, T. Baum, N. Kao, S.N. Bhattacharya, Dielectric properties and electromagnetic interference shielding effectiveness of graphene-based biodegradable nanocomposites, *Materials & Design*, 109 (2016) 68-78.
- [40] S. Kang, S. Qiao, Z. Hu, J. Yu, Y. Wang, J. Zhu, Interfacial polymerized reduced graphene oxide covalently grafted polyaniline nanocomposites for high-performance electromagnetic wave absorber, *Journal of Materials Science*, 54 (2019) 6410-6424.
- [41] S. Azizi, É. David, M.F. Fréchet, C.M. Ouellet-Plamondon, Numerical simulation of the effective permittivity of low-density polyethylene composite filled by carbon black, *IET Nanodielectrics*, (2019).
- [42] R.S. Kurusu, E. Helal, N. Moghimian, E. David, N. Demarquette, The Role of Selectively Located Commercial Graphene Nanoplatelets in the Electrical Properties, Morphology, and Stability of EVA/LLDPE Blends, *Macromolecular Materials and Engineering*, (2018) 1800187.
- [43] S. Azizi, E. David, M.F. Fréchet, P. Nguyen Tri, C.M. Ouellet-Plamondon, Electrical and thermal phenomena in low-density polyethylene/carbon black composites near the percolation threshold, *J. Appl. Polym. Sci.*, (2018) 47043.
- [44] T.T. Anh, M. Fréchet, É. David, R. Veillette, P. Moraille, Effect of POSS-grafted titanium dioxide on the electrical and thermal properties of LDPE/TiO₂ polymer nanocomposite, *J. Appl. Polym. Sci.*, 135 (2018) 46095.
- [45] S.J. He, J.B. Hu, C. Zhang, J.Q. Wang, L. Chen, X.M. Bian, J. Lin, X.Z. Du, Performance improvement in nano-alumina filled silicone rubber composites by using vinyl tri-methoxysilane, *Polym. Test.*, 67 (2018) 295-301.
- [46] Y. Xue, X.-f. Li, D.-h. Zhang, H.-s. Wang, Y. Chen, Y.-f. Chen, Comparison of ATH and SiO₂ fillers filled silicone rubber composites for HTV insulators, *Compos. Sci. Technol.*, 155 (2018) 137-143.
- [47] A.K. Bhowmick, J. Konar, S. Kole, S. Narayanan, Surface-Properties of Epdm, Silicone-Rubber, and Their Blend during Aging, *J. Appl. Polym. Sci.*, 57 (1995) 631-637.
- [48] M. Su, X. Zeng, X. Lai, H. Li, Effect of mixing sequences of γ -piperazine propylmethyl dimethoxysilane on the tracking and erosion resistance of silicone rubber, *Polym. Test.*, 65 (2018) 491-496.

- [49] Y. Lin, L. Wang, F. Yin, M. Farzaneh, Y. Liu, S. Gao, Comparison of four commonly used high temperature vulcanized silicone rubber formulas for outdoor insulator and their regional adaptability, *J. Appl. Polym. Sci.*, (2019) 47477.
- [50] T.K.B. Sharmila, J.V. Antony, M.P. Jayakrishnan, P.M.S. Beegum, E.T. Thachil, Mechanical, thermal and dielectric properties of hybrid composites of epoxy and reduced graphene oxide/iron oxide, *Materials & Design*, 90 (2016) 66-75.
- [51] S. Azizi, C. Ouellet-Plamondon, E. David, M. Fréchet, Electric Response and Thermal Properties of Ethylene Vinyl Acetate/Graphene-based Composite, *IEEE*, (2018).
- [52] S. Akhlaghi, A.M. Pourrahimi, C. Sjöstedt, M. Bellander, M.S. Hedenqvist, U.W. Gedde, Degradation of fluoroelastomers in rapeseed biodiesel at different oxygen concentrations, *Polym. Degrad. Stab.*, 136 (2017) 10-19.
- [53] S. Akhlaghi, A. Pourrahimi, C. Sjöstedt, M. Bellander, M. Hedenqvist, U. Gedde, Effects of ageing conditions on degradation of acrylonitrile butadiene rubber filled with heat-treated ZnO star-shaped particles in rapeseed biodiesel, *Polym. Degrad. Stab.*, 138 (2017) 27-39.
- [54] T.H. Mokhothu, A.S. Luyt, M. Messori, Preparation and characterization of EPDM/silica nanocomposites prepared through non-hydrolytic sol-gel method in the absence and presence of a coupling agent, *Express Polymer Letters*, 8 (2014) 809-822.
- [55] M. Ali, M.A. Choudhry, Preparation and characterization of EPDM-silica nano/micro composites for high voltage insulation applications, *Materials Science-Poland*, 33 (2015) 213-219.
- [56] F. Yan, X. Zhang, F. Liu, X. Li, Z. Zhang, Adjusting the properties of silicone rubber filled with nanosilica by changing the surface organic groups of nanosilica, *Composites Part B: Engineering*, 75 (2015) 47-52.
- [57] L. Gan, S. Shang, S.-x. Jiang, Impact of vinyl concentration of a silicone rubber on the properties of the graphene oxide filled silicone rubber composites, *Composites Part B: Engineering*, 84 (2016) 294-300.
- [58] Z. Boussaboun, S. Azizi, C. Ouellet-Plamondon, Conductive clay containing graphene layers, *Nanotechnology (IEEE-NANO)*, 2017 IEEE 17th International Conference on, IEEE, 2017, pp. 1065-1069.
- [59] C. Zhang, K. Pal, J.U. Byeon, S.M. Han, J.K. Kim, A Study on Mechanical and Thermal Properties of Silicone Rubber/EPDM Damping Materials, *J. Appl. Polym. Sci.*, 119 (2011) 2737-2741.
- [60] Y. Liu, Y. Shi, D. Zhang, J. Li, G.J.P. Huang, Preparation and thermal degradation behavior of room temperature vulcanized silicone rubber-g-polyhedral oligomeric silsesquioxanes, 54 (2013) 6140-6149.
- [61] M.T. Nazir, B. Phung, M. Hoffman, S. Yu, S. Li, Micro-AlN/nano-SiO₂ co-filled silicone rubber composites with high thermal stability and excellent dielectric properties, *Mater. Lett.*, 209 (2017) 421-424.
- [62] E.S. Kim, E.J. Kim, J.H. Shim, J.S.J.J.o.a.p.s. Yoon, Thermal stability and ablation properties of silicone rubber composites, 110 (2008) 1263-1270.

- [63] Z. Han, A. Fina, Thermal conductivity of carbon nanotubes and their polymer nanocomposites: a review, *Prog. Polym. Sci.*, 36 (2011) 914-944.
- [64] J. Song, C. Chen, Y. Zhang, Manufacturing, High thermal conductivity and stretchability of layer-by-layer assembled silicone rubber/graphene nanosheets multilayered films, *Composites Part A: Applied Science*, 105 (2018) 1-8.
- [65] B. Gorelov, A. Gorb, A. Nadtochiy, D. Starokadomsky, V. Kuryliuk, N. Sigareva, S. Shulga, V. Ogenko, O. Korotchenkov, O. Polovina, Epoxy filled with bare and oxidized multi-layered graphene nanoplatelets: a comparative study of filler loading impact on thermal properties, *Journal of Materials Science*, 54 (2019) 9247-9266.
- [66] S. Azizi, E. David, M.F. Fréchet, P. Nguyen-Tri, C. Ouellet-Plamondon, Electrical and thermal conductivity of ethylene vinyl acetate composite with graphene and carbon black filler, *Polym. Test.*, (2018).
- [67] C.L. Huang, X. Qian, R.G. Yang, Thermal conductivity of polymers and polymer nanocomposites, *Materials Science & Engineering R-Reports*, 132 (2018) 1-22.
- [68] N. Burger, A. Laachachi, M. Ferriol, M. Lutz, V. Toniazzi, D. Ruch, Review of thermal conductivity in composites: mechanisms, parameters and theory, *Prog. Polym. Sci.*, 61 (2016) 1-28.
- [69] Y.Z. Song, J.H. Yu, L.H. Yu, F.E. Alam, W. Dai, C.Y. Li, N. Jiang, Enhancing the thermal, electrical, and mechanical properties of silicone rubber by addition of graphene nanoplatelets, *Materials & Design*, 88 (2015) 950-957.
- [70] E. Vazirinasab, R. Jafari, G. Momen, Application of superhydrophobic coatings as a corrosion barrier: A review, *Surf. Coat. Technol.*, 341 (2018) 40-56.
- [71] G. Momen, M. Farzaneh, Survey of micro/nano filler use to improve silicone rubber for outdoor insulators, *Rev. Adv. Mater. Sci.*, 27 (2011) 1-13.

Highlights

- EPDM and silicone (S) rubbers were compounded with titanium dioxide (TiO_2), modified fumed silica (MFS) and graphene (G) additives *via* mechanical mixing.
- The thermal stability of the EPDM and EPDM/silicone rubber composites was increased.
- The dielectric breakdown strength of the EPDM composites was increased by additives loading.
- TGA-FTIR analysis revealed the thermal degradation of the rubber composites.
- Utilizing TiO_2 , MFS and graphene additives appeared to mitigate the destructive incidents in HV insulating materials.

Dear **Prof. Gedde**,

Department of Department of Fibre and Polymer Technology

Editor-in-Chief: **Polymer Testing Journal**,

There are no conflicts of interest among the following authors:

1. Sohrab Azizi
2. Gelareh Momen
3. Claudiane Ouellet-Plamondon
4. Eric David

Sincerely yours,

Sohrab Azizi, Ph.D.

AUTHORSHIP STATEMENT

Manuscript entitled "Performance Improvement of EPDM and EPDM/Silicone Rubber Composites Using Modified Fumed Silica, Titanium Dioxide and Graphene additives"

All of the authors listed in this manuscript certify that they have been participated closely in the current research study. In more details: all of the authors have contributed in implementing the test plan. Dr. Sohrab Azizi has run the experimental plan and acquiring the data. All authors participated in analyzing and discussing the data. The manuscript has been written by the first authors and reviewed and revised by the other authors. All authors certify that none of the materials used for this study has not been used in another research study and will not be used or published in the future in another research study before publishing in Polymer Testing Journal.

*Sincerely yours,
Sohrab Azizi, Ph.D.*

*Department of Automation and production Engineering
École de technologie supérieure (Université du Québec)
1100 Notre-Dame St W, Montreal, QC H3C 1K3 Canada*